THE JOURNAL OF PHYSICAL CHEMISTRY B

Article

pubs.acs.org/JPCB

Protonation and Anion Binding Control the Kinetics of Iron Release from Human Transferrin

Rajesh Kumar[†,‡] and A. Grant Mauk*[,†]

[†]Department of Biochemistry and Molecular Biology and the Centre for Blood Research, Life Sciences Centre, 2350 Health Sciences Mall, University of British Columbia, Vancouver, BC V6T 1Z3 Canada

[‡]School of Chemistry and Biochemistry, Thapar University, Patiala 147004, India

Supporting Information

ABSTRACT: Iron release in vitro from human serum diferric transferrin (hFe_2Tf) in acidic media ($4.2 \leq pH \leq 5.4$) in the presence of nonsynergistic anions occurs in at least five kinetic steps. Step 1 (most rapid) involves proton assisted release of carbonate from the protein. In subsequent steps, iron release from both the N- and C-terminal lobes is controlled by slow proton transfers and anion binding. In step 2, the N-terminal lobe takes up one proton with kinetic linkage to the binding of one anion. In step 3, iron release from the anion-linked N-terminal lobe is controlled by slow uptake of two protons with rate-constant, k_{2N}, of $2.6(6) \times 10^7$, $6.1(6) \times 10^7$, and $9(1) \times 10^7$ M^{-2} s^{-1} in the presence of Cl^-, NO_3^-, and SO_4^{2-}, respectively. In step 4, the C-terminal lobe takes up one proton with kinetic linkage to the binding of one anion. In step 5, iron release from the anion-linked C-terminal lobe is controlled by slow uptake of two protons with rate-constant, k_{2C}, of $8.4(2) \times 10^4$, $4.4(6) \times 10^5$, and $8.1(2) \times 10^5$ M^{-2} s^{-1} in the presence of Cl^-, NO_3^-, and SO_4^{2-}, respectively.

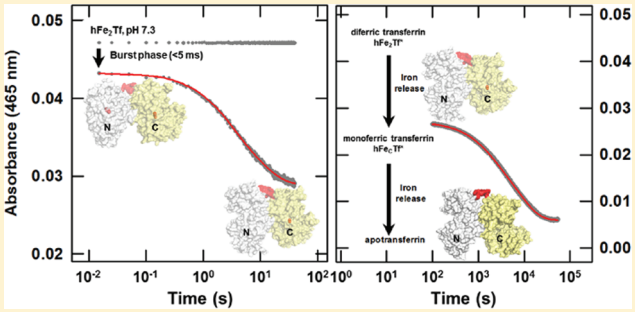

INTRODUCTION

Transferrins (Tfs; serum transferrin (sTf), ovotransferrin (oTf), and lactoferrin (Lf)) are a family of bilobed iron-binding glycoproteins[1] with extremely high affinities for iron ($K_a \approx 10^{20}$ M^{-1}).[2] This high affinity for iron affords protection against iron-catalyzed free radical formation and limits bacterial access to iron in the host circulation. Tfs also bind nonferrous metal ions, some of which are of therapeutic and diagnostic interest.[3−6] sTf has the additional, critical role of transporting iron from the gut, liver and spleen to cells that require it. Cellular uptake of the sTf-Fe complex involves receptor-mediated endocytosis that leads to dissociation of the complex at endosomal pH (pH ∼5.5).[7−11] Increasing evidence indicates that several anions (e.g., ATP, citrate, Cl^-) occurring in millimolar concentrations in the cytosol[12] and other non-physiological anions (e.g., sulfate, nitrate, perchlorate) may facilitate the uptake and release of iron by sTf[13] and that they interact with sTf through specific binding sites.[14−19] Nevertheless, the mechanism by which these anions regulate the uptake and release of iron by sTf is not clearly understood.

Human sTf consists of a single polypeptide chain (679 residues, ∼80 kDa) that folds as two globular domains, the N-lobe and the C-lobe, with a short peptide chain connecting them.[20,21] Each lobe coordinates one iron atom through four highly conserved residues: one aspartyl, one histidyl, and two tyrosyl residues. In addition, the iron atom is also coordinated to a synergistic carbonate anion,[22−24] without which the protein loses its affinity for the metal.[24−28] In the absence of bound iron, the two lobes assume an open conformation, and the binding of iron results in a closed conformation.[27−31] Moreover, binding of iron results in formation of several interdomain hydrogen bonds in each lobe.[32,33] These hydrogen bonds differ both between the members of the transferrin family and between the two lobes of a given transferrin.[32−35] The hydrogen bonds formed at the entrance to the iron binding cleft control the access of water from bulk solvent to the iron binding site and constitute a trigger for the cleft opening.[25,26,35,36]

Although, the overall structures of the N- and C-lobes are quite similar, the two domains differ in their (a) affinity for iron and the mechanism by which their binding of iron is regulated,[37,38] (b) conformational and thermal stability,[6,39,40] (c) interaction with nonsynergistic anions,[41] and (d) kinetics of iron binding and release.[42−46] Physiologically, low molecular weight synthetic chelators play an important role in the iron exchange reactions with sTf, and the rate of iron release from the N-lobe is approximately twice that of the C-lobe in both the full-length molecule and in the separated, half-molecule domains.[46,47] Although detailed molecular origins of these differences are not fully understood, one significant structural and mechanistic difference between the two domains has been identified.

Received: June 22, 2011
Revised: February 16, 2012
Published: February 24, 2012

   dx.doi.org/10.1021/jp205879h | J. Phys. Chem. B 2012, 116, 3795−3807

Specifically, the *N*-lobe possesses two lysyl residues (Lys[206] and Lys[296]) located opposite each other on the two opposing faces of the cleft that is apparent in the structure of the apoprotein. With iron bound, these residues form an H-bond with each other in an arrangement known as the "dilysine trigger" that was first identified in the structure of oTf[35] but also occurs in the structure of sTf.[48,49] Interaction of these two residues was proposed to be responsible for the release of iron from the N-lobe at relatively high pH.[35] The C-lobe of sTf lacks a similar pair of lysyl residues and releases its iron at lower pH. On the other hand, the C-lobe possesses a kinetically significant anion-binding site (KISAB) in the C-lobe that is absent from the N-lobe.[35,46,50] Addition of simple nonsynergistic anions such as chloride accelerates the chelator-mediated iron release from Tfs and differentially affects the thermodynamic and kinetic behavior of the metal binding sites.[51−58] Folajtar and Chasteen reported that two anions bind to each domain of diferric transferrin (hFe_2Tf).[18] Various anions affect the EPR spectrum of hFe_2Tf similarly, indicating that they do not coordinate directly to the iron atoms but possibly bind to cationic residues (e.g., lysyl residues) or the positive dipoles of helix N-termini located near the metal ion-binding sites.[18,19,59,60] Recently, site-directed mutagenesis of N- and C-terminal monoferric transferrin has implicated a role for Lys[296] and Lys[569] in anion binding.[46,61,62]

Considerable interest has been focused on delineating the mechanism of iron release from Tfs in vitro through use of small molecular weight chelators[43−47,50,61−64] combined with pH-jump methods[10,25,26,65−67] in the presence and absence of the sTf receptor.[10,65,68−70] Recent reports emphasize that in the absence of nonsynergistic anions, the slow protonation of iron-binding residues of hFe_2Tf controls the iron release process at mildly acidic pH.[10,42,65,67] To investigate the effect of anions on the pH-dependent process of iron release and, in particular, to evaluate the mechanism by which anion binding and the slow protonation of iron-binding residues regulate iron release at the mildly acidic pH range characteristic of endosomes, we have analyzed the effects of anions on the kinetics of iron release from human diferric transferrin (hFe_2Tf) under these conditions in the absence of chelators and the receptor. Particular attention has been paid to chemical relaxation analysis of the kinetics of iron release from hFe_2Tf. The results provide evidence that protonation and interaction of anions with the iron-binding residues of each lobe of sTf control the kinetics of iron release.

EXPERIMENTAL METHODS

Diferric transferrin (T0665) and apotransferrin (T2252) were purchased from Sigma. NaCl, Na_2SO_4, and sodium acetate were from Fisher. HEPES and MES were from Acros and Sigma, respectively. HEPES, MES, and acetate buffers of the desired concentration were prepared by dissolving the anhydrous salt in glass distilled water that had been polished with a Barnstead Nanopure purification system, and pH was adjusted with 1 M NaOH or acetic acid. The concentration of hFe_2Tf was determined spectrophotometrically ($\varepsilon_{465nm} = 5 \times 10^3\ M^{-1}\ cm^{-1}$).[2,71] The commercial diferric transferrin was dissolved in Hepes buffer (50 mM, pH 7.4). This buffer was exchanged with fresh buffer 4−5 times by centrifugal ultrafiltration (Centricon ultrafilter (Millipore), 10 000-Da molecular mass cutoff). The resulting solutions exhibited a well-defined band at 280 nm, and an A_{465nm}/A_{280nm} ratio of ∼0.046 that is characteristic of human transferrin fully saturated with iron.[72−74]

C-terminal monoferric transferrin was produced by incubation of apotransferrin with exactly one equivalent freshly prepared iron nitrilotriacetate. Apotransferrin (81 mg, 1 μmol) was dissolved in HEPES buffer (100 mM, pH 7.4, 20 mM $NaHCO_3$, 50 mM NaCl). An iron nitrilotriacetate solution was prepared by dissolving $FeCl_3{\cdot}6H_2O$ (15 μmol) and nitriloacetic acid (30 μmol) in 6 M HCl (2 mL), adjusting to pH 4.0 with NaOH solution, and diluting to 10 mL. Apotransferrin (200 μM) was incubated with iron nitrilotriacetate solution (200 μM; 5 h, 37 °C). The resulting transferrin solution was exchanged into the desired buffer by centrifugal ultrafiltration (Centricon ultrafilter (Millipore), 10 000-Da molecular mass cutoff) to remove nitrilotriacetate. The concentration of the C-site iron-loaded transferrin was determined spectrophotometrically ($\varepsilon_{465nm} = 2.5 \times 10^3\ M^{-1}\ cm^{-1}$).[2,45,71]

Electronic Absorption Spectra of hFe_2Tf as a Function of pH and Anion Concentration. Solutions of hFe_2Tf (∼8 μM) were prepared in chloride- (0.0, 0.04, 0.15, 0.8, and 1.2 M) or sulfate- (0.013, 0.1, and 0.25 M) containing HEPES (0.05 M, pH 7.3−5.4) or sodium acetate buffer (0.01 M, pH 4.75−4.2). Samples were incubated for 10−15 h at 25 °C prior to spectrum acquisition with a Cary model 6000i spectrophotometer equipped with a Peltier accessory at 25.0(1) °C.

Kinetics Measurements. Manual mixing kinetics experiments were performed by thorough mixing of a neutral aqueous solution of hFe_2Tf with acetate (pH ≤ 4.75) or MES (pH ≥ 5.3) buffers containing varying concentrations of NaCl, $NaNO_3$, and Na_2SO_4 to achieve a final pH of 4.2−5.4 (Mettler SevenMulti pH meter), final [acetate] and [MES] values of 10 μM and 50 mM, respectively, and a final [hFe_2Tf] of 8−10 μM. The resulting change in absorbance at 465 nm was monitored with a Cary Model 6000i spectrophotometer (25.0 ± 0.1 °C).

Stopped-Flow Kinetics Measurements. Rapid mixing experiments were performed with a BioLogic (SFM 400 mixing module) stopped-flow spectrophotometer equipped with a thermostatted bath (25.0(5) °C) by mixing a neutral aqueous solution of hFe_2Tf with acetate buffer (pH ≤ 4.75) containing various concentrations of NaCl and Na_2SO_4 and monitoring the change in absorbance at 465 nm. Typically, 4−6 reaction traces were averaged. The final pH was in the range 4.2−4.75, the final acetate buffer concentration was 10 mM, and the final protein concentration was 8 μM.

Data Analysis. The kinetics data collected manually or by stopped-flow spectroscopy were analyzed with the programs SigmaPlot (v. 10) and BioKine (Biologic), respectively. The analysis of relaxation kinetics data was based on the procedure reported by El Hage Chahine and co-workers,[42,66,67,75,76] and the derivations of the rate expressions used for this analysis are provided in the Supporting Information. Many experiments required conditions of varying ionic strength to 0.5 M or higher. We have analyzed the ionic strength dependence of kinetics data obtained at ionic strengths up to than 0.5 M based on the demonstration by Pitzer[77,78] that Debye−Hückel theory performs surprisingly well up to ionic strengths at least this great, if not greater.

RESULTS

Electronic Absorption Spectra of hFe_2Tf as a Function of pH and Anion Concentration. The dependence of the visible electronic spectrum of the hFe_2Tf complex on pH (4.2−7.4) and anions used in the present study is shown in Figure 1a. At pH 7.4, the spectrum of hFe_2Tf exhibits an absorbance maximum (465 nm) that is associated with bound

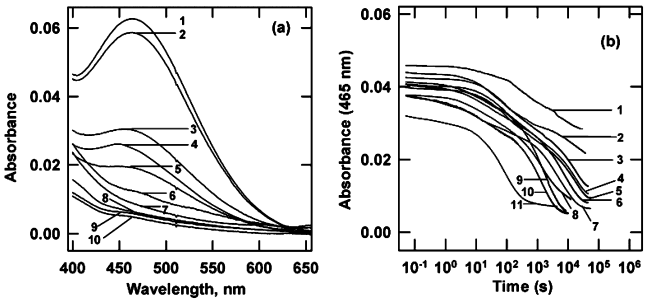

Figure 1. pH-dependent electronic absorption spectroscopy of hFe_2Tf in the presence of varying concentrations of chloride and sulfate. (a) Electronic absorption spectra of hFe_2Tf as a function of pH, buffer and anion content. Absorbance spectra 1−10 correspond to the following conditions: (1−3) HEPES buffer (0.05 M) pH 7.3, 6.0, and 5.4, respectively; (4 and 5) sodium acetate buffer (0.01 M) pH 4.75 and pH 5.4 with chloride (0.8 M), respectively; (6−10) sodium acetate buffer (0.01 M) pH 4.75 with 0.15 M chloride, pH 4.75 with 0.01 M sulfate, and pH 4.55 with 0.04 M chloride, and pH 4.2 with 0.04 M chloride, respectively. (b) Kinetics of iron release from hFe_2Tf (monitored at 465 nm). Iron release kinetic traces 1−11 correspond to the following conditions: (1, 3−5, and 7) HEPES buffer (0.05 M, pH 5.4) with no additions, 0.8 M chloride, 1.2 M chloride, 0.013 M sulfate, respectively; (2, 6, 8, and 9) sodium acetate buffer (0.01 M, pH 4.75) with no additions, 0.1 M sulfate, 0.15 M chloride, 1.2 M chloride, 0.013 M sulfate, 0.04 M chloride, respectively; and (10 and 11) sodium acetate buffer (0.01 M, pH 4.55) with 0.04 M chloride and 1.2 M chloride, respectively.

iron and is independent of pH near neutrality (7.4−6.0). As pH is decreased from 6.0 to 4.2, absorbance at 465 nm decreases, consistent with pH-dependent release of iron from hFe_2Tf. Lowering pH from 4.55 to pH 4.2 eliminates this maximum and releases iron completely. Notably, the pH-dependence of this absorbance varies with the anionic composition of the solution. Chloride (0.15 M) or sulfate (0.013 M) eliminate absorbance at 465 nm at higher pH (~4.75) (Figure 1a). At greater chloride (0.8 M) or sulfate (0.1 M) concentrations, this absorbance is almost completely eliminated at even higher pH (~5.4; Figure 1a). In the absence of anions, the N-lobe begins to release iron as pH is lowered to ~5.7 while the C-lobe retains iron until pH is lowered to ~4.8.[79,80] The pH-dependent anion effects on the spectrum of hFe_2Tf (Figure 1a) suggest that anions induce the C-lobe to start releasing iron between pH 5.4 and 4.8.

Kinetics of Iron Release from hFe_2Tf as a Function of pH and Anion Concentration. These pH-dependent anion effects also influence the kinetics of iron release from hFe_2Tf (Figure 1b). Notably, lower $[SO_4^{2-}]$ and $[NO_3^-]$ are required to achieve the same effect observed only at higher $[Cl^-]$. We have characterized this effect further by evaluating the kinetics of iron release from hFe_2Tf in the presence and absence of these three anions at pH 4.2 to 5.4.

In mildly acidic media in the presence of chloride or sulfate, the release of iron from hFe_2Tf exhibits biphasic kinetics (Figure 1b and Figure 2c (inset)) following a burst phase

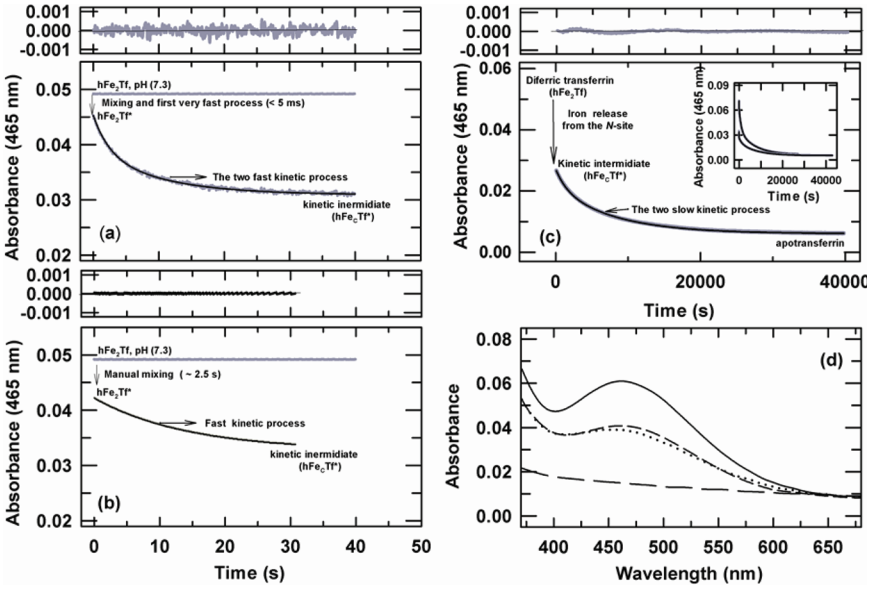

Figure 2. Kinetics of iron release from hFe_2Tf (~8 μM) monitored at 465 nm on decreasing pH from 7.3 to 4.5 in the presence of acetate buffer (10 mM) containing 0.045 M chloride (25 °C). (a) A representative stopped-flow kinetic trace for the rapid phase (0−40 s) of iron release. The kinetics are best described by two relaxation processes (residuals shown in upper panel) with time constants of ~2.4 and ~13.6 s. The absorbance of a control sample (pH 7.3, no pH-jump) is also shown. (b) The manual mixing time when monitoring kinetics by conventional spectrophotometry is ~2.5 s, and for processes occurring 0.1−30 s after manual mixing, the data are best described by a single-exponential fit (residuals shown in upper panel) with the time constant $\tau_{2N} \approx 14.2$ s. (c) A representative trace of the slow phase ($70-6 \times 10^5$ s) of iron release under identical conditions. The kinetics of this phase are best described by two relaxation processes (residuals shown in upper panel) with time constants of $\sim 1.5 \times 10^3$ and $\sim 8.1 \times 10^3$ s. The inset shows the kinetic traces ($2-6 \times 10^5$ s) following manual mixing (~1 s) for ~8 μM (lower curve) and for ~16 μM (upper curve) protein. These kinetic traces are best fitted as three exponential processes with time constants, $\tau_{2N} \approx 17$ s, $\tau_{3C} \approx 1500$ s, and $\tau_{4C} \approx 7834$ s (upper curve) and $\tau_{2N} \approx 20$ s, $\tau_{3C} \approx 1450$ s, and $\tau_{4C} \approx 7875$ s (lower curve). (d) Visible absorption spectra of various transferrin species (~10 μ M) (25 °C). Long-dash, solid, and dotted-lines represent the spectra of apotransferrin, diferric-transferrin, and C-site only iron-loaded transferrin, respectively (pH ~7.4, 0.1 M HEPES with 0.045 M NaCl). The short-dash line represents the visible spectrum of the C-site only iron-loaded transferrin measured rapidly following pH jump of hFe_2Tf from neutrality to pH 4.5 [sodium acetate buffer (10 mM) with NaCl (0.45 M)] before the beginning of the slow kinetic phenomenon in panel c. The spectrum of the only C-site iron-loaded transferrin (dotted line) coincides with that measured at the end of the processes in panel a and before the beginning of the processes in panel c.

dx.doi.org/10.1021/jp205879h | J. Phys. Chem. B 2012, 116, 3795−3807

(Figure 2a). As shown (Figure 2a), absorbance at 465 nm decreases from 5 ms to 100 s after decreasing pH from 7 to 4.55 by mixing with acetate buffer (~8 mM) containing chloride (0.04 M). At ~8 μM protein, an overall absorption variation for the first kinetic phase is about 0.02 (Figure 2b). The noise and drift relevant to the signals monitored during our stopped flow kinetics measurements were significantly lower than the changes in amplitudes that we measured; therefore, the values of the overall absorption variations we reported for the iron loss from the N-lobe are meaningful. The mixing time of our stopped-flow apparatus is 3−5 ms, so the relaxation times that fall within this period cannot be analyzed. This burst phase (<5 ms) may involve proton-assisted release of the synergistic carbonate anion in acidic media because carbonate release is a prerequisite for iron release (eq 1)[26,66,67]

$$hFe_2Tf + nH \rightleftharpoons hFe_2Tf^* \text{ or } hFe_{NC}Tf^* + CO_2/(HCO_3^-) \quad (1)$$

where hFe_2Tf is transferrin with both Fe^{3+} and carbonate bound and $hFe_{NC}Tf^*$ is the same protein without carbonate bound. Both forms of the protein are in an unknown state of protonation.

Nevertheless, for processes occurring 5 ms-100 s after mixing, the data are best described by a two-exponential fit with the time constants $\tau_{1N} \sim 2.4$ s and $\tau_{2N} \approx 13.6$ s (Figure 2a). For processes occurring 0.1−100 s after manual mixing (dead time ~2.5 s), the data are best described by a single-exponential fit with the time constant $\tau_{2N} \approx 14.2$ s (Figure 2b). The processes responsible for these kinetic phases are related to release of iron from the N-lobe of $hFe_{NC}Tf^*$ because in mildly acidic media, iron release from this form of the protein occurs first from the N-lobe and then from the C-lobe.[10,67] Moreover, at pH < 5.4, the spectrum measured at the end of the processes in Figure 2a and before the beginning of the processes in Figure 2c is always of the C-site transferrin iron complex in acidic media (Figure 2d). Therefore, the processes in Figure 2a are related to the N-lobe only. After ~100 s, absorbance at 465 nm continues to decrease in a biexponential manner with time constants $\tau_{3C} \approx 0.43$ h and $\tau_{4C} \approx 2.3$ h (Figure 2c). These two processes are ascribed to iron release from the C-lobe. The time dependence of iron release from the carbonate-free N-lobe of $hFe_{NC}Tf^*$ and the C-lobe of hFe_CTf^* were determined as a function of $[Cl^-]$, $[SO_4^{2-}]$, and $[NO_3^-]$ at pH ~4.55 (Figure 3 panels a and d, b and e, and the insets of b and e, respectively). Fitting these results to eq 2 (for $hFe_{NC}Tf^*$, Figure 3a,d), eq 2a (for $hFe_{NC}Tf^*$, insets of Figure 3b,e) and eq 3 (for hFe_CTf^*, Figure 3b,e) by nonlinear, least-squares analysis provides the lifetimes for these processes that were used to determine their dependences on $[Cl^-]$, $[NO_3^-]$, and $[SO_4^{2-}]$ (Figure 3, panels c and f and insets of c and f) at pH 4.55.

$$A_t = B + A_1 \exp\left(-\frac{t}{\tau_{1N}}\right) + A_2 \exp\left(-\frac{t}{\tau_{2N}}\right) \quad (2)$$

$$A_t = B + A_2 \exp\left(-\frac{t}{\tau_{2N}}\right) \quad (2a)$$

$$A_t = B + A_3 \exp\left(-\frac{t}{\tau_{3C}}\right) + A_4 \exp\left(-\frac{t}{\tau_{4C}}\right) \quad (3)$$

As $[Cl^-]$ or $[NO_3^-]$ is increased from 0.04 to 0.5 M or as $[SO_4^{2-}]$ is increased from 0.002 to 0.13 M, iron is released more rapidly from both $hFe_{NC}Tf^*$ and hFe_CTf^*. The inverse of the time constants for the first phase of iron release from $hFe_{NC}Tf^*$ (τ_{1N}^{-1}, Figure 3c) and hFe_CTf^* (τ_{3C}^{-1}, Figure 3f) increased almost linearly with $[Cl^-]$, $[NO_3^-]$, and $[SO_4^{2-}]$, whereas the corresponding values for the second phase of iron release from $hFe_{NC}Tf^*$ (τ_{2N}^{-1}, Figure 3c (inset)) and hFe_CTf^* (τ_{4C}^{-1}, Figure 3f (inset)) exhibited simple monoexponential variation with $[Cl^-]$, $[NO_3^-]$, and $[SO_4^{2-}]$. Overall, these results establish that sulfate has a greater effect on increasing the rate of iron release from hFe_2Tf than does chloride or nitrate (Figure 3, panels c and f and their insets). Over the pH range of 4.2−5.4, similar dependences of τ_{1N}^{-1} and τ_{3C}^{-1} on $[Cl^-]$ (Figure 4a,c), $[NO_3^-]$ (Figure 4e) and $[SO_4^{2-}]$ (Figure 5a,c) are observed while τ_{2N}^{-1}, and τ_{4C}^{-1} increase monoexponentially with $[Cl^-]$ (Figure 4b,d), $[NO_3^-]$ (Figure 4f), and $[SO_4^{2-}]$ (Figure 5b,d). These observations warranted a chemical relaxation analysis of the kinetic processes responsible for the pH-induced iron release from hFe_2Tf (pH 4.2−5.4) as a function of $[Cl^-]$, $[NO_3^-]$, and $[SO_4^{2-}]$.

Chemical Relaxation Analysis of Proton-Linked Iron Release from hFe_2Tf (pH 4.2−5.4) as a Function of $[Cl^-]$, $[NO_3^-]$, and $[SO_4^{2-}]$. As indicated above, on lowering the pH of a solution of hFe_2Tf from neutrality to pH 4.2−5.4, the first and fastest process occurs within the dead-time of the stopped-flow mixer (<5 ms), and we attribute this process to proton-assisted loss of the synergistic carbonate anion (Figure 2a and eq 1). The carbonate-free protein, $hFe_{NC}Tf^*$, subsequently releases iron in two kinetically detectable steps: a fast step (step 2) and a slow step (step 3) (Figure 2a). The fast step can be treated as a relaxation process.[75,76] If we assume that in this step $hFe_{NC}Tf^*$ binds an anion from solution and binds a proton under diffusion control,[75] two mechanisms are possible. The first mechanism involves the binding of a proton followed by binding of an anion (eqs 4 and 5, where S represents an anion)

$$hFe_{NC}Tf^* + H^+ \rightleftharpoons hFe_{NC}Tf^*H \quad (4)$$

$$hFe_{NC}Tf^*H + S \underset{k_{-1N}}{\overset{k_{1N}}{\rightleftharpoons}} hFe_{NC}Tf^*SH \quad (5)$$

with $K_{1H} = [hFe_{NC}Tf^*][H^+]/[hFe_{NC}Tf^*H]$ and $K_{1S} = [hFe_{NC}Tf^*H][S]/[hFe_{NC}Tf^*SH]$. When eq 5 is assumed to be rate limiting, then the reciprocal relaxation time associated with eq 5 can be expressed as eq 5a (see Supporting Information)

$$\tau_{1N}^{-1} = k_{-1N} + \{k_{1N}([H^+][S])/K_{1H}\} \quad (5a)$$

The second possible mechanism involves binding of an anion followed by binding of a proton (eqs 6 and 7)

$$hFe_{NC}Tf^* + S \underset{k'_{-1N}}{\overset{k'_{1N}}{\rightleftharpoons}} hFe_{NC}Tf^*S \quad (6)$$

$$hFe_{NC}Tf^*S + H^+ \rightleftharpoons hFe_{NC}Tf^*SH \quad (7)$$

with $K'_{1S} = [hFe_{NC}Tf^*][S]/[hFe_{NC}Tf^*S]$ and $K'_{1H} = [hFe_{NC}Tf^*S][H^+]/[hFe_{NC}Tf^*SH]$. If the reaction described by eq 6 is rate limiting, the reciprocal relaxation time associated with eq 6 can be expressed as eq 6a (see Supporting Information)

$$\tau'^{-1}_{1N} = k'_{1N}[S] + \{K'_{1H}k'_{-1N}/([H^+] + K'_{1H})\} \quad (6a)$$

Of these two options, only the first is consistent with the experimental data (Figure 6a,b). For each anion, the values of k_{1N}/K_{1H} and k_{-1N} are determined from the slopes and intercepts

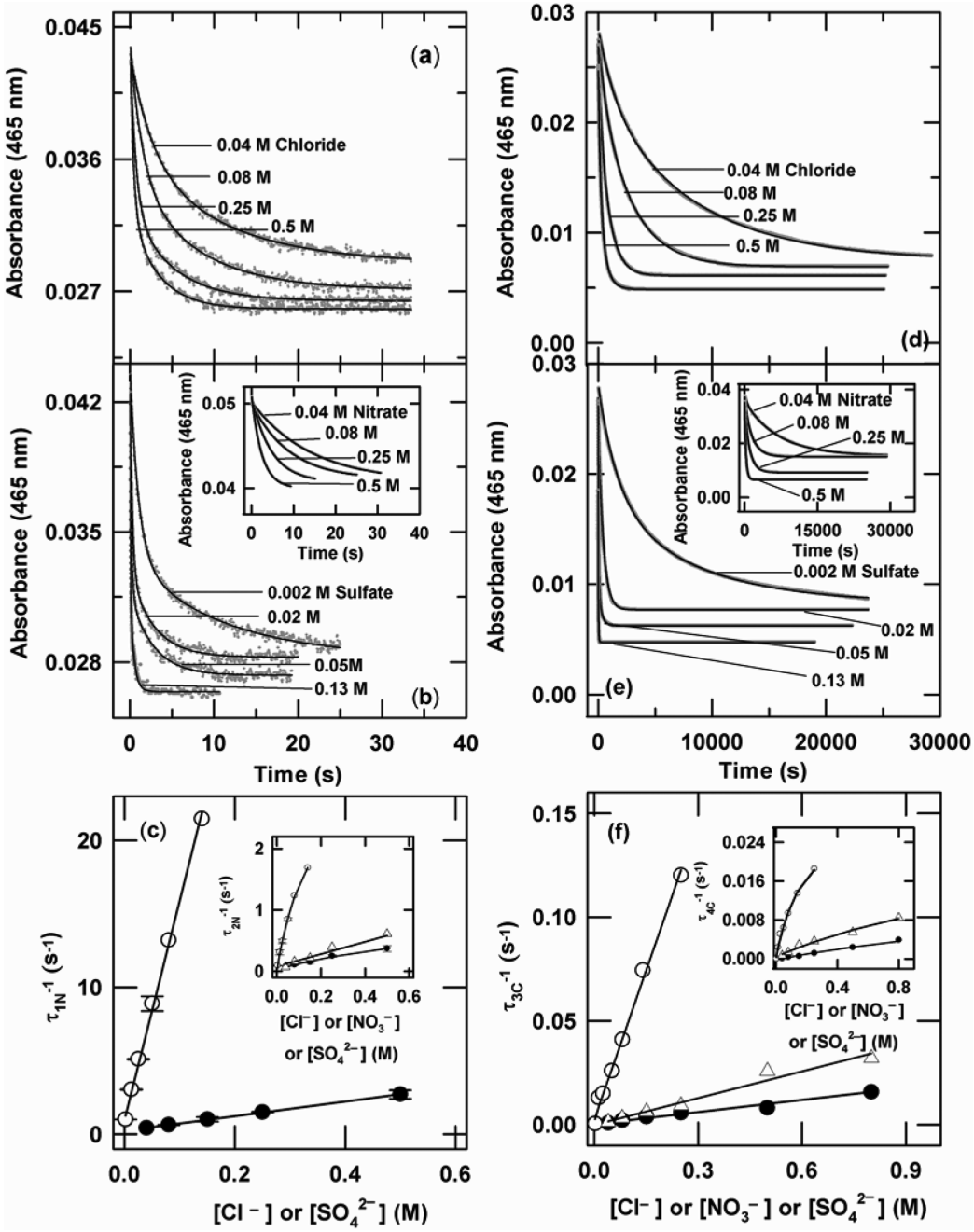

Figure 3. Dependence of kinetics of iron release from hFe_2Tf on [Cl^-], [SO_4^{2-}], and [NO_3^-] (25 °C, pH ~4.55). Panels a and b present the rapid phase of iron release (from the N-site of hFe_2Tf) following stopped-flow pH-jump from 7.3 to 4.55 at various [Cl^-] and [SO_4^{2-}], respectively. The solid lines represent least-squares fits of the data to a biexponential function that produce the time constants, τ_{1N} and τ_{2N} that are plotted as a function of [Cl^-] or [SO_4^{2-}], respectively, in panel c and its inset. The solid lines in panel c represent the linear least-squares fits to the data, and solid lines in the inset of panel c are nonlinear least-squares fits to the data. The error bars indicate the standard deviations of the τ_{1N} and τ_{2N} values plotted. Panels d and e present the slow phase of iron release (from the C-site of hFe_2Tf) for experiments described in panels a and b, and the inset of panel b. The resulting time constants, τ_{3C} and τ_{4C}, are plotted as a function of [Cl^-], [SO_4^{2-}] and [NO_3^-] in panel f and its inset; the solid lines in panel f are linear least-squares fits to the data, and the solid lines in the inset of panel f are nonlinear least-squares fits to the data.

derived from fitting the data to eq 5a as shown for Cl^- and SO_4^{2-} in Figure 6, panels a and b (Table 1), respectively. This result suggests that $hFe_{NC}Tf^*$ first binds one proton and then binds an anion to form the kinetic intermediate $hFe_{NC}Tf^*SH$.

Dissociation of iron from the $hFe_{NC}Tf^*SH$ intermediate occurs next (step 3). In considering this process, it is useful to consider all mechanisms by which $hFe_{NC}Tf^*SH$ can protonate, interact with anions and release Fe(III). Only the following processes are consistent with our experimental observations

$$hFe_{NC}Tf^*SH \underset{k'_{-2N}}{\overset{k'_{2N}}{\rightleftharpoons}} hFe_CTf^*SH + Fe \quad (8)$$

dx.doi.org/10.1021/jp205879h | J. Phys. Chem. B 2012, 116, 3795−3807

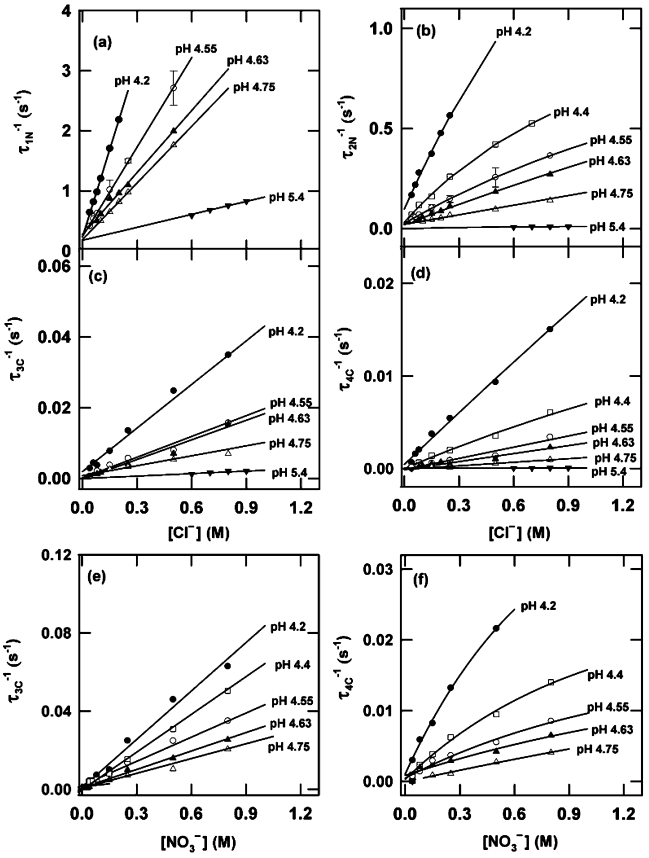

Figure 4. Dependence of kinetics of iron release from the N- and C-lobes of hFe_2Tf on pH and [Cl^-] or [NO_3^-]. Panels a and b show the dependence of the reciprocal relaxation times, τ_{1N}^{-1} and τ_{2N}^{-1}, for iron release from the N-site of hFe_2Tf on [Cl^-] at (●) pH 4.2, (□) 4.4, (○) 4.55, (▲) 4.63, (Δ) 4.75, and (▼) 5.4. The error bars indicate the standard deviations, the solid lines in panel a are fits to a linear function, and in panel b they represent nonlinear least-squares fits of the data to a single-exponential. Panels c and d show the dependence of the reciprocal relaxation times, τ_{3C}^{-1} and τ_{4C}^{-1}, for iron release from the C-site of hFe_2Tf on [Cl^-] at pH (●) 4.2, (□) 4.4, (○) 4.55, (▲) 4.63, (Δ) 4.75, and (▼) 5.4 The solid lines in panel c are fits of the data to a linear function, and in panel d they represent nonlinear least-squares fits of the data to a single-exponential. Panels e and f show the dependence of the reciprocal relaxation times, τ_{3C}^{-1} and τ_{4C}^{-1}, for iron release from the C-site of hFe_2Tf on [NO_3^-] at pH (●) 4.2, (□) 4.4, (○) 4.55, (▲) 4.63, and (Δ) 4.75.The solid lines in panel e are fits of the data to a linear function, and in panel f they represent nonlinear least-squares fits of the data to a single-exponential.

$$hFe_CTf^*SH + 2H^+ \underset{k_{-2N}}{\overset{k_{2N}}{\rightleftharpoons}} hFe_CTf^*SH_3 \quad (9)$$

$$hFe_CTf^*SH_3 \underset{k''_{-2N}}{\overset{k''_{2N}}{\rightleftharpoons}} hFe_CTf^* + S \quad (10)$$

To determine which of these processes is rate limiting, we analyzed our data with the assumption any one of them could be rate limiting and found that only by assuming that eq 9 is rate limiting could our data be fitted successfully (see the Supporting Information, Figure 6, and Table 2). If the reaction described by eq 9 is assumed to be rate-limiting, then the equation that describes the reciprocal relaxation time for this reaction (eq 11) pertains

$$\tau_{2N}^{-1} = k_{-2N}([S]/K_{2S}) + k_{2N(obs)}[H^+]^2 \quad (11)$$

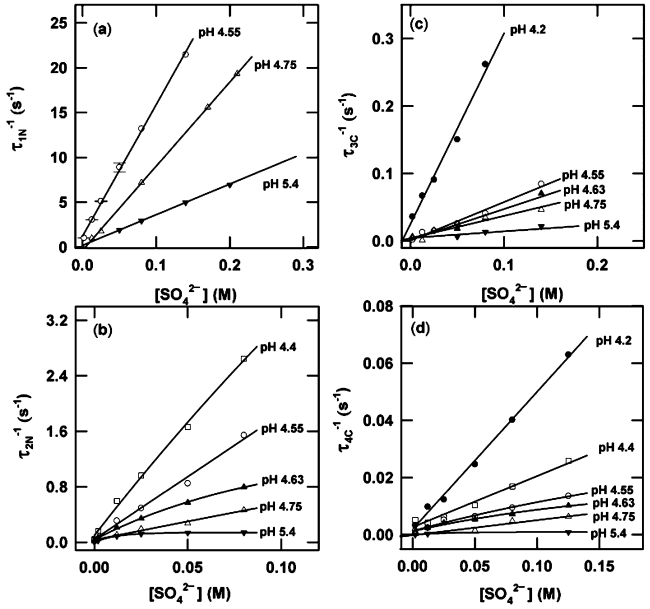

Figure 5. pH and [SO_4^{2-}] dependence of kinetics of iron release from the N- and C-lobes hFe_2Tf. Panels a and b show the dependence of the reciprocal relaxation times, τ_{1N}^{-1} and τ_{2N}^{-1}, for iron release from the N-site on [SO_4^{2-}] at (●) pH 4.2, (□) 4.4, (○) 4.55, (▲) 4.63, (Δ) 4.75, and (▼) 5.4. Error bars denote standard deviations. The solid lines in panel a are fits of the data to a linear function, whereas the solid lines in panel b represent nonlinear least-squares fit of the data to a single-exponential. Panels c and d show the dependence of the reciprocal relaxation times, τ_{3C}^{-1} and τ_{4C}^{-1}, for iron release from the C-site of hFe_2Tf on [SO_4^{2-}] at (●) pH 4.2, (□) 4.4, (○) 4.55, (▲) 4.63, (Δ) 4.75, and (▼) 5.4. The solid lines in panel c are fits of the data to a linear function, whereas the solid lines in panel d represent nonlinear least-squares fits of the data to a single-exponential.

and under our experimental conditions ($4.2 \leq pH \leq 5.4$)

$$k_{2N(obs)} = k_{2N} + k_{2N}[S]/K_{2S} \quad (12)$$

At constant [S] (when S is Cl^-, NO_3^-, or SO_4^{2-}), the reciprocal relaxation times associated with eq 11 observed in our experiments are linearly dependent on $[H^+]^2$ (Figure 6c, Table 2; Figure 6d, Table 2; and Figure 6e, Table 2, respectively). The slopes determined for each [S] from linear regression fits to eq 11 provide $k_{2N(obs)}$ (Figure 6c,d,e), and k_{2N} and k_{2N}/K_{2S} are determined from the intercepts and slopes of linear fitting of data to eq 12 [Figure 6f and its inset (Table 2)]. Values of equilibrium constant K_{2S} for Cl^-, NO_3^-, and SO_4^{2-} are calculated from the values of k_{2N} and k_{2N}/K_{2S} obtained for Cl^-, NO_3^-, and SO_4^{2-}, respectively (Table 2). This result demonstrates that iron release from $hFe_{NC}Tf^*SH$ is controlled by a slow gain of two protons as described by eqs 8−10.

With formation of the intermediate hFe_CTf^*, in which iron is bound (without carbonate) to the C-lobe only, another series of processes ensues that culminates in formation of apo-Tf. Iron release from hFe_CTf^* takes place in two kinetically detectable steps (Figures 2c and 3d,e and inset of Figure 3e). The faster component can be treated as a relaxation process.[75,76] If we assume that in this step hFe_CTf^* binds a proton (at the diffusion limit[75]) and interacts with an anion from solution, two mechanisms can be envisaged. In the first mechanism, hFe_CTf^* binds one proton and then binds an anion

$$hFe_CTf^* + H^+ \rightleftharpoons hFe_CTf^*H \quad (13)$$

dx.doi.org/10.1021/jp205879h | J. Phys. Chem. B 2012, 116, 3795−3807

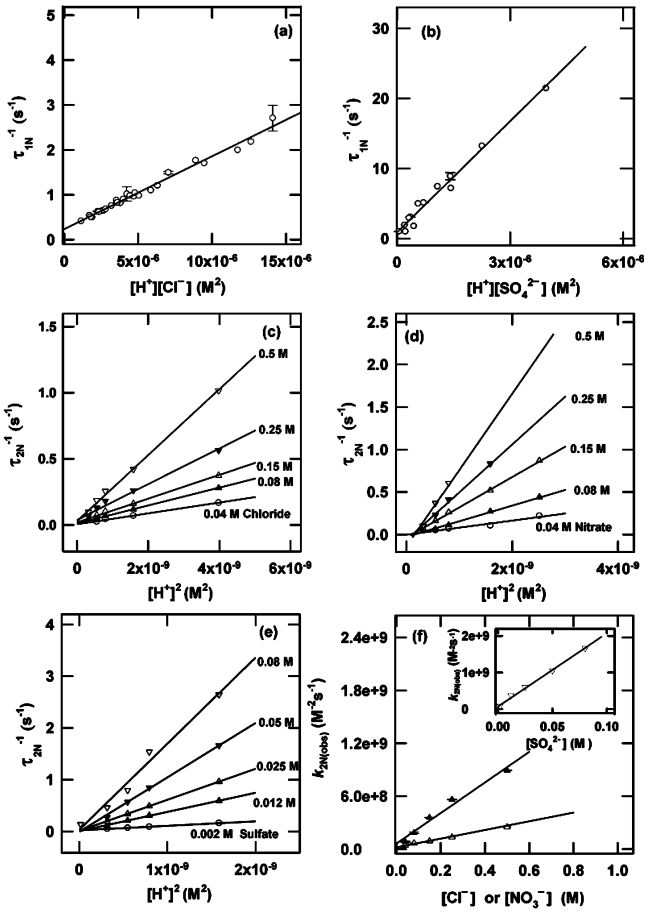

Figure 6. Relaxation kinetics analysis of iron release from $hFe_{NC}Tf^*$ as a function of pH, $[Cl^-]$, $[SO_4^{2-}]$, and $[NO_3^-]$ (25 °C). Panel a shows the dependence of τ_{1N}^{-1} for iron release from the N-lobe on $[H^+][Cl^-]$ for $4.2 \le pH \le 5.4$, with $0.04\ M \le [Cl^-] \le 0.5\ M$. The values of τ_{1N}^{-1} in panel a were determined at several values of pH (4.2, 4.55, 4.63, 4.75, and 5.4) as a function of $[Cl^-]$. Error bars denote standard deviations. The linear least-squares fit of the data in panel (a) (solid line) yields an intercept of 0.24(4) s^{-1}, a slope of $1.62(4) \times 10^5$ $M^{-2}s^{-1}$ and $r = 0.985$. Panel b shows the dependence of τ_{1N}^{-1} on $[H^+][SO_4^{2-}]$ for $4.2 \le pH \le 5.4$, with $0.002\ M \le [SO_4^{2-}] \le 0.2\ M$. The values of τ_{1N}^{-1} in panel b were determined at several values of pH (4.55, 4.75, and 5.4) as a function of $[SO_4^{2-}]$. The linear least-squares fit of the data in the inset of panel a (solid line) yields an intercept of 0.8(2) s^{-1}, a slope of $5.3(2) \times 10^6$ M^{-2} s^{-1} and $r = 0.981$, Panels c and d show the dependence of τ_{2N}^{-1} on $[H^+]^2$ at constant $[Cl^-]$ and $[NO_3^-]$ for $4.2 \le pH \le 5.4$, respectively. The slopes of the regression fits of the data to eq 11 at constant $[Cl^-]$ (panel c) and $[NO_3^-]$ (panel d) are plotted as a function of $[Cl^-]$ (Δ) and $[NO_3^-]$ (▲) in panel f. Panel e shows the dependence of τ_{2N}^{-1} on $[H^+]$ at constant $[SO_4^{2-}]$ for $4.2 \le pH \le 5.4$. The slopes of the regression fits of the data to eq 11 at constant $[SO_4^{2-}]$ (panel e) are plotted as a function of $[SO_4^{2-}]$ in the inset of panel f. The linear least-squares fit of the data for chloride in panel f (solid line) yields an intercept of 2.6 (6) $\times 10^7$ M^{-2} s^{-1}, a slope of $4.5(2) \times 10^8$ $M^{-3}s^{-1}$ and $r = 0.998$. The linear least-squares fit of the data for nitrate in panel f (solid line) yields an intercept of 6.1 (6) $\times 10^7$ M^{-2} s^{-1}, a slope of $1.7(2) \times 10^9$ M^{-3} s^{-1} and $r = 0.977$. The linear least-squares fitting of the data for sulfate in the inset of panel f (solid line) yields an intercept of $9(1) \times 10^7$ M^{-2} s^{-1} and a slope of 1.97 (6) $\times 10^{10}$ M^{-3} s^{-1}. In these analyses, only those values of τ_{1N}^{-1} and τ_{2N}^{-1} obtained under conditions of pH and anion concentration that the iron bound to the N-lobe of hFe_2Tf is released completely were considered.

Table 1. Values of k_{1N}/K_{1H}, k_{-1N}, k_{1C}/K_{1H}, and k_{-1C} at 25.0(5) °C[a]

anion	k_{1N}/K_{1H} (M^{-1} s^{-1})	k_{-1N} (s^{-1})	k_{1C}/K_{1H} (M^{-1} s^{-1})	k_{-1N} (s^{-1})
Cl^-	$1.62(4) \times 10^5$	0.24(4)	$7.34(1) \times 10^2$	$0.2(1) \times 10^{-5}$
SO_4^{2-}	$5.3(2) \times 10^6$	0.80(2)	$1.72(3) \times 10^4$	$0.5(1) \times 10^{-4}$
NO_3^-			$1.43(1) \times 10^3$	$0.6(1) \times 10^{-5}$

[a]The uncertainty (standard error) of the least significant figure is indicated in parentheses.

Table 2. Second Order Rate Constants k_{2N} and Equilibrium Constant K_{2S} at 25.0(5) °C[a]

anion	k_{2N} (M^{-2} s^{-1})	K_{2S} (M)	K_a (M^{-1})
Cl^-	$2.6(6) \times 10^7$	$5.78(3) \times 10^{-2}$	17.3
SO_4^{2-}	$9(1) \times 10^7$	$4.57(4) \times 10^{-3}$	219
NO_3^-	$6.1(6) \times 10^7$	$3.59(3) \times 10^{-2}$	27.85

[a]The uncertainty (standard error) of the least significant figure is indicated in parentheses.

$$hFe_CTf^*H + S \underset{k_{-1C}}{\overset{k_{1C}}{\rightleftharpoons}} Fe_CTf^*SH \quad (14)$$

where $K_{1H} = [hFe_CTf^*][H^+]/[hFe_CTf^*H]$ and $K_{1S} = [hFe_CTf^*H][S]/[hFe_CTf^*SH]$. The reciprocal relaxation time associated with eq 14 when eq 14 is assumed to be rate-limiting can be expressed as eq 14a

$$\tau_{3C}^{-1} = k_{-1C} + \{k_{1C}([H^+][S])/K_{1H}\} \quad (14a)$$

In the second mechanism, hFe_CTf^* first binds an anion and then binds a proton

$$hFe_CTf^* + S \underset{k'_{-1C}}{\overset{k'_{1C}}{\rightleftharpoons}} Fe_CTf^*S \quad (15)$$

$$hFe_CTf^*S + H^+ \rightleftharpoons Fe_CTf^*SH \quad (16)$$

The equilibrium constants for these reactions are $K'_{1S} = [hFe_CTf^*][S]/[hFe_CTf^*S]$ and $K'_{1H} = [hFe_CTf^*S][H^+]/[hFe_CTf^*SH]$. If the equilibrium represented by eq 15 is assumed to be rate-limiting, then the reciprocal relaxation time associated with eq 15 can be expressed as eq 15a.

$$\tau'^{-1}_{3C} = k'_{1C}[S] + \{K'_{1H}k'_{-1C}/([H^+] + K'_{1H})\} \quad (15a)$$

Only the first of these two possibilities is consistent with the experimental data (Figure 6a,b and inset of Figure 6a). For each anion, the values of k_{1C}/K_{1H} and k_{-1C} are determined from the slopes and intercepts of the regression line (eq 14a) as shown for Cl^-, SO_4^{2-}, and NO_3^- in Figure 7a (Table 1), Figure 7b (Table 1), and inset of Figure 7a (Table 1), respectively.

With formation of hFe_CTf^*SH, the final stage of iron dissociation from the C-lobe begins. As for the corresponding species discussed above ($hFe_{NC}Tf^*SH$), hFe_CTf^*SH can protonate and bind an anion prior to dissociation of iron as described by the following reactions:

$$hFe_CTf^*SH \underset{k'_{-2C}}{\overset{k'_{2C}}{\rightleftharpoons}} hTf^*SH + Fe \quad (17)$$

dx.doi.org/10.1021/jp205879h | J. Phys. Chem. B 2012, 116, 3795−3807

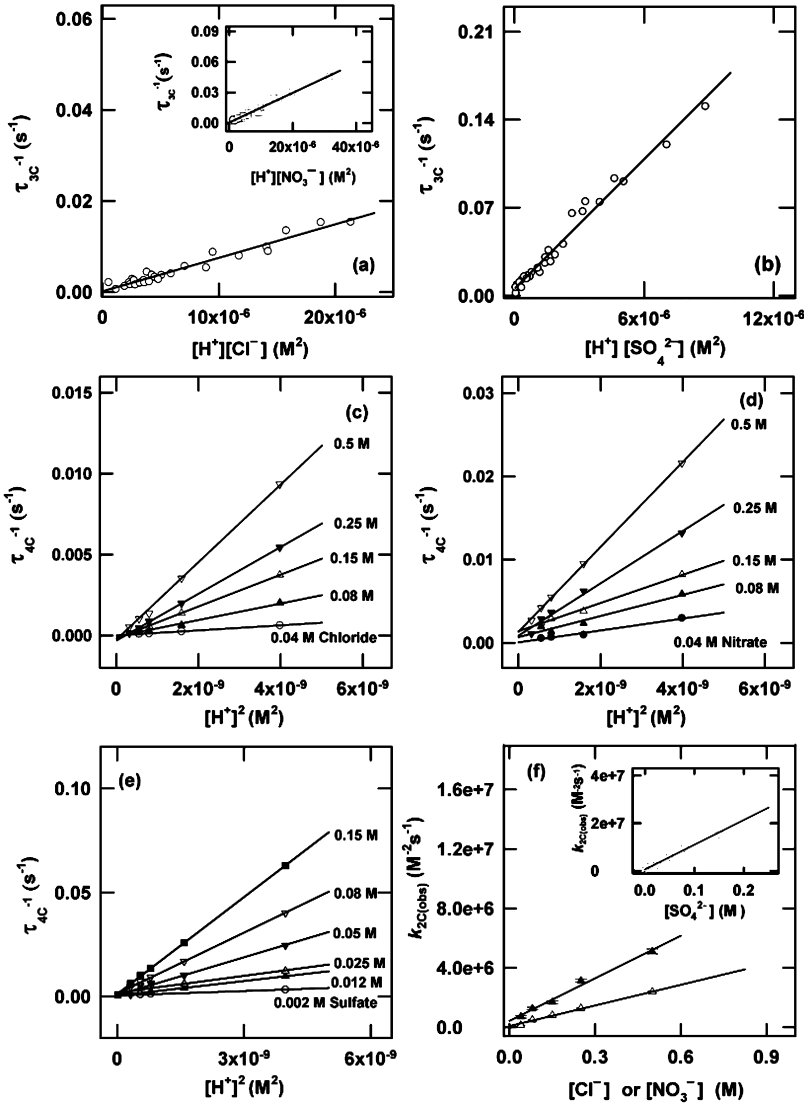

Figure 7. Relaxation kinetics analysis of iron release from hFe_CTf*SH as a function of [pH, $[Cl^-]$, $[SO_4^{2-}]$, and $[NO_3^-]$ (25 °C). Panel a shows the dependence of τ_{3C}^{-1} for iron release from the C-lobe on $[H^+][Cl^-]$ for $4.2 \leq pH \leq 4.75$, with $0.04\ M \leq [Cl^-] \leq 0.5\ M$. The values of τ_{3C}^{-1} in panel a were determined at various fixed values of pH (4.2, 4.55, 4.63, 4.75, and 5.4) and varying $[Cl^-]$. The linear least-squares fit of these data (solid line) yields an intercept of $0.2(1) \times 10^{-5}\ s^{-1}$ and a slope of $7.34(1) \times 10^2\ M^{-1}\ s^{-1}$ with $r = 0.96$. Inset: Dependence of τ_{3C}^{-1} on $[H^+][NO_3^-]$ for $4.2 \leq pH \leq 4.75$, with $0.04\ M \leq [NO_3^-] \leq 0.5\ M$. The values of τ_{3C}^{-1} in the inset were determined at various fixed values of pH (4.2, 4.55, 4.63, and 4.75) and varying $[NO_3^-]$. The linear least-squares fit of these data (solid line) yields an intercept of $0.6(1) \times 10^{-5}\ s^{-1}$ and a slope of $1.45(3) \times 10^3\ M^{-1}\ s^{-1}$ with $r = 0.98$. Panel b shows the dependence of τ_{3C}^{-1} on $[H^+][SO_4^{2-}]$ for $4.2 \leq pH \leq 5.4$, with $0.002\ M \leq [SO_4^{2-}] \leq 0.2\ M$. The values of τ_{3C}^{-1} in panel b were determined at various fixed pH values (4.2, 4.55, 4.63, 4.75, and 5.4) and varying sulfate concentration. The linear least-squares fit of these data (solid line) yields an intercept of $0.5(1) \times 10^{-4}\ s^{-1}$, a slope of $1.72(3) \times 10^4\ M^{-1}\ s^{-1}$ and $r = 0.98$. Panels c and d show the dependence of τ_{4C}^{-1} on $[H^+]^2$ as a function of $[Cl^-]$ and $[NO_3^-]$ for $4.2 \leq pH \leq 5.4$, respectively. Panel f reports the slopes of the regression fits of the data in Panels c and d to eq 20 as a function of (Δ) $[Cl^-]$ (panel c) and (▲) $[NO_3^-]$ (panel d). The linear least-squares fit of the data for chloride yields an intercept of $8.4(6) \times 10^4\ M^{-2}\ s^{-1}$ and a slope of $4.6(6) \times 10^6\ M^{-3}\ s^{-1}$ with $r = 0.998$. Corresponding analysis of the data for nitrate yields an intercept of $4.4(6) \times 10^5\ M^{-2}\ s^{-1}$, a slope of $9.6(2) \times 10^6\ M^{-3}\ s^{-1}$ and $r = 0.988$. Panel e shows the dependence of τ_{4C}^{-1} on $[H^+]^2$ as a function of $[SO_4^{2-}]$, $4.2 \leq pH \leq 5.4$. The dependence of the slopes obtained from fitting these data to eq 20 as a function of $[SO_4^{2-}]$ is shown in the inset of panel f. The linear least-squares fitting of the data for sulfate in the inset of panel f (solid line) yields an intercept of $8(1) \times 10^5\ M^{-2}\ s^{-1}$ and a slope of $1.01\ (6) \times 10^8\ M^{-3}\ s^{-1}$. In these analyses only those values of τ_{3C}^{-1} and τ_{4C}^{-1} obtained under conditions of pH and anion concentration that the iron bound to the C-lobe of hFe_2Tf is released completely are considered.

$$hTf^*SH + 2H^+ \underset{k_{-2C}}{\overset{k_{2C}}{\rightleftharpoons}} hTf^*SH_3 \quad (18)$$

$$hTf^*SH_3 \underset{k''_{-2C}}{\overset{k''_{2C}}{\rightleftharpoons}} hTf^*H_3 + S \quad (19)$$

Fitting our experimental data to the equations describing the reciprocal relaxation times related to eqs 17− 19 when each is considered rate-limiting led to an acceptable fit only for the case in which the reaction described by eq 18 is rate limiting (see the Supporting Information, Figure 7, and Table 2). Thus, the equation describing the reciprocal relaxation time for this reaction (eq 20) is of use

$$\tau_{2C}^{-1} = k_{-2C}([S]/K_{2S}) + k_{2C(obs)}[H^+]^2 \quad (20)$$

dx.doi.org/10.1021/jp205879h | J. Phys. Chem. B 2012, 116, 3795−3807

Scheme 1. Mechanism of Iron Release from hFe_2Tf in the Absence of the Receptor

Step 1 (most rapid, < 5 ms) involves pH-linked carbonate release from hFe_2Tf.

$$hFe_2Tf + nH \rightleftharpoons hFe_2Tf^* \text{ or } hFe_{NC}Tf^* + CO_2/(HCO_3^-) \quad (A)$$

In step 2, the N-site gains one proton with kinetic linkage to the binding of one anion (S)

$$hFe_{NC}Tf^* + H^+ \rightleftharpoons hFe_{NC}Tf^*H \quad (B)$$

$$hFe_{NC}Tf^*H + S \underset{k_{-1N}}{\overset{k_{1N}}{\rightleftharpoons}} hFe_{NC}Tf^*SH \quad (C)$$

In step 3, iron is released from $hFe_{NC}Tf^*SH$ according to Eqs. (D) to (E)

$$hFe_{NC}Tf^*SH \underset{k'_{-2N}}{\overset{k'_{2N}}{\rightleftharpoons}} hFe_CTf^*SH + Fe \quad (D)$$

$$hFe_{NC}Tf^*SH + 2H^+ \underset{k_{-2N}}{\overset{k_{2N}}{\rightleftharpoons}} hFe_CTf^*SH_3 \quad (E)$$

$$hFe_CTf^*SH_3 \underset{k''_{-2N}}{\overset{k''_{2N}}{\rightleftharpoons}} hFe_CTf^* + S \quad (F)$$

In step 4, the C-lobe gains one proton with kinetic linkage to the binding of one anion

$$hFe_CTf^* + H^+ \rightleftharpoons hFe_CTf^*H \quad (G)$$

$$hFe_CTf^*H + S \underset{k_{-1C}}{\overset{k_{1C}}{\rightleftharpoons}} Fe_CTf^*SH \quad (H)$$

In step 5, iron is released from hFe_CTf^*SH according to Eqs. (I) to (K)

$$hFe_CTf^*SH \underset{k'_{-2C}}{\overset{k'_{2C}}{\rightleftharpoons}} hTf^*SH + Fe \quad (I)$$

$$hTf^*SH + 2H^+ \underset{k_{-2C}}{\overset{k_{2C}}{\rightleftharpoons}} hTf^*SH_3 \quad (J)$$

$$hTf^*SH_3 \underset{k''_{-2C}}{\overset{k''_{2C}}{\rightleftharpoons}} hTf^*H_3 + S \quad (K)$$

and under our experimental conditions ($4.2 \leq pH \leq 5.4$)

$$k_{2C(obs)} = k_{2C} + k_{2C}[S]/K_{2S} \quad (21)$$

At constant [S] (when S is Cl^-, NO_3^-, or SO_4^{2-}), the experimental reciprocal relaxation times associated with eq 20 are linear with respect to $[H^+]^2$ (Figure 7c, Table 2; Figure 7d, Table 2; and Figure 7e, Table 2, respectively). The slopes determined for each [S] from linear regression fits to eq 20 provide $k_{2C(obs)}$ (Figure 7c,d,e), and k_{2C} and k_{2C}/K_{2S} are determined from the intercepts and slopes of linear fitting of data to eq 21 (Figure 7f and inset, Table 2). Values of equilibrium constant K_{2S} for Cl^-, NO_3^-, and SO_4^{2-} are derived from the values of k_{2C} and k_{2C}/K_{2S} obtained for Cl^-, NO_3^- and SO_4^{2-}, respectively (Table 2). This result demonstrates that iron release from hFe_CTf^*SH is controlled by slow binding of two protons according to eqs 17−19.

DISCUSSION

While the analysis we provide here has not been undertaken previously for human transferrin, a similar study has been reported for another member of this protein family, lactoferrin.[66] In the presence of anions at mildly acidic pH comparable to that found in the endosome (pH ~4.2−5.4), iron is released from hFe_2Tf according to the sequence of reactions outlined in Scheme 1. Although the net result of this process is very similar to that for iron release from diferric lactoferrin (Fe_2Lf), it is notable that more of the individual steps in this sequence of reactions are kinetically detectable for iron release from transferrin than for iron release from lactoferrin (Scheme 2).[64] Specifically, dissociation of iron from hFe_2Tf occurs first from the N-lobe to yield a kinetically detectable intermediate with iron bound to the C-lobe only. This intermediate is not detected in the case of iron loss from Fe_2Lf under similar conditions.[66]

Scheme 2. Mechanism of Iron Release from Fe_2Lf

Step 1 (most rapid, < 5 ms) involves pH-linked carbonate release from Fe_2Lf.

$$Fe_2Lf + nH \rightleftharpoons Fe_2Lf^* \text{ or } Fe_{NC}Lf^* + CO_2/(HCO_3^-) \quad (A)$$

In step 2, the Fe_2Lf binds two protons with kinetic linkage to the binding of two monoanions (i.e., Cl^-) or one dianion (i.e., SO_4^{2-}).

$$Fe_2Lf^* + 2H^+ \rightleftharpoons Fe_2Lf^*H_2 \quad (B)$$

$$Fe_2Lf^*H_2 + nS \underset{k_{-1N}}{\overset{k_{1N}}{\rightleftharpoons}} Fe_2Lf^*S_nH_2 \quad (C)$$

In step 3, iron is released from $Fe_2Lf^*S_nH_2$ according to Eqs. (D) to (E)

$$Fe_2Lf^*S_nH_2 \underset{k'_{-2N}}{\overset{k'_{2N}}{\rightleftharpoons}} Lf^*S_nH_2 + 2Fe \quad (D)$$

$$Lf^*S_nH_2 + 2H^+ \underset{k_{-2N}}{\overset{k_{2N}}{\rightleftharpoons}} Lf^*S_nH_4 \quad (E)$$

$$Lf^*S_nH_4 \underset{k''_{-2N}}{\overset{k''_{2N}}{\rightleftharpoons}} Lf^*H_4 + nS \quad (F)$$

Whether the loss of the synergistic carbonate from each lobe of Fe_2Tf occurs during the initial rapid release of iron from hFe_2Tf cannot be determined unambiguously. Nevertheless, as carbonate release is essential for iron dissociation from hFe_2Tf,[26,66,67] it most probably occurs during the first kinetic step. During release of iron from the N-lobe, rapid liberation of carbonate is followed by binding of one proton and the exposure of an anion interaction site (eq 4). The N-lobe then binds an anion, consistent with the presence of a specific site of electrostatic interaction (eq 5). Although the identity of the anion binding site remains to be determined, Lys^{206}, Lys^{296}, and Arg^{124} are likely possibilities.[48,61,62,81] Notably, site-directed mutagenesis of the isolated N-lobe of sTf has implicated a role

dx.doi.org/10.1021/jp205879h | J. Phys. Chem. B 2012, 116, 3795−3807

Scheme 3. Mechanism of Iron Release from hFe_2Tf in the Presence of the Receptor

Step 1 (most rapid, < 5 ms) involves pH-linked carbonate release from the *N*-site of hFe_2Tf-TR

$$hFe_2Tf\text{-}TR + nH \rightleftharpoons hFe_2Tf^*\text{-}TR \text{ or } hFe_{NC}Tf^*\text{-}TR + CO_2/(HCO_3^-) \quad (A)$$

In step 2, the rate of iron loss from the *N*-site of $hFe_{NC}Tf^*$-TR is controlled by slow uptake of one proton followed by more rapid uptake of two additional protons.

$$hFe_{NC}Tf^*\text{-}TR + H^+ \rightleftharpoons hFe_{NC}Tf^*H\text{-}TR \quad (B)$$
(rate – limiting)

$$hFe_NTf^*H\text{-}TR \underset{k_{-1N}}{\overset{k_{1N}}{\rightleftharpoons}} hFe_CTf^*H\text{-}TR + Fe_N^{3+} \quad (C)$$

$$hFe_CTf^*H\text{-}TR + 2H^+ \underset{k_{-1N}}{\overset{k_{1N}}{\rightleftharpoons}} hFe_CTf^*H_3\text{-}TR \quad (D)$$
(diffusion – controlled)

Step 3 involves pH-linked carbonate release from the *C*-site, i.e., $hFe_CTf^*H_3$-TR

$$hFe_CTfH_3^*\text{-}TR + nH \rightleftharpoons hFe_CTfH_3^{**}\text{-}TR + CO_2/(HCO_3^-) \quad (E)$$

In step 4, the rate of iron loss from the *C*-site (*i.e.*, $hFe_CTfH_3^{**}$-TR) is controlled by slow uptake of one proton followed by more rapid uptake of two protons.

$$hFe_CTfH_3^{**}\text{-}TR + H^+ \rightleftharpoons hFe_CTfH_4^{**}\text{-}TR \quad (F)$$
(rate – limiting)

$$hFe_CTfH_4^{**}\text{-}TR \underset{k_{-1N}}{\overset{k_{1N}}{\rightleftharpoons}} hTfH_4^{**}\text{-}TR + Fe_C^{3+} \quad (G)$$

$$hTfH_4^{**}\text{-}TR + 2H^+ \underset{k_{-1N}}{\overset{k_{1N}}{\rightleftharpoons}} hTfH_6^{**}\text{-}TR \quad (H)$$
(diffusion – controlled)

for Lys^{296} in anion interaction.[61] In general, this type of electrostatic interaction is diffusion-controlled. We note that the dependence of the reciprocal relaxation time, τ_{2N}^{-1}, on anion concentration (Figure 6a,b and eq 11) does not necessarily result from the binding of an anion but could also result from a protein conformational change that kinetically controls ion-binding.

The kinetic product generated upon loss of iron bound to the N-lobe (eq 8) undergoes two rate-limiting proton transfers (eq 9) and, finally, releases an anion (eq 10). Classical proton transfers are typically diffusion controlled and occur within microseconds.[75,83] In the case of transferrin, we assume, therefore, that these proton transfers are controlled by slow changes in the conformation of the protein, which can explain the dependence of eqs 11 and 20 on $[H^+]^2$. This possibility has also been proposed for the slow proton transfers observed during iron loss from lactoferrin,[66] serum transferrin,[67] and ovotransferrin.[26] These findings suggest that at mildly acidic pH and in the presence of anions, loss of iron from the N-lobe requires electrostatic binding of one anion, presumably involving Lys^{296}, and three protons for protonation of the of the Tyr^{95} and Tyr^{188} phenolate groups and the imidazole group of His^{249}.[42,67,82] This sequence of events does not exclude concomitant protonation of other sites on transferrin.

An intermediate, hFe_CTf^*, with iron bound only at the C-lobe (Scheme 1), is produced following release of the anion associated with dissociation of iron from the N-lobe. This intermediate binds one proton and then an anion (eq 13), possibly at a site involving Lys^{569}.[46] The intermediate product resulting from anion binding releases the iron (eq 17), undergoes two rate-limiting proton transfers (eq 18), and ultimately releases an anion (eq 19). In general, classical proton transfers are diffusion-controlled and in an acidic medium usually occur within microseconds.[75,76,83] We assume, therefore, that in the case of iron release from the N- and C-lobe, the slow proton transfers and anion binding processes we observe are under kinetic control of protein conformational changes. A similar interpretation has been proposed for the slow proton transfers and anion binding processes observed during dissociation of iron from Lf.[66] Notably, a recent report comparing the mechanisms of iron release by sTf, oTf, and Lf concludes that at ionic strength ≤0.5 M, iron loss from Lf occurs at pH < 3.5 and is always preceded by partial unfolding of the protein while neither sTf nor oTf undergo unfolding-induced iron release in this range of ionic strength and mildly acidic conditions.[66]

Another useful comparison permitted by the current results concerns the effect that binding to the receptor has on iron release from hFe_2Tf. At present, this comparison is compromised by divergent views of the mechanism by which iron dissociates from the hFe_2Tf–receptor complex.[10,67,84] In the presence of the receptor, El Hage Chahine et al. have reported a mechanism for iron release from hFe_2Tf in mildly acidic medium (Scheme 3)[10] in which iron release is independent of ionic strength for μ < 0.5.[42,65] However, the current results clearly demonstrate that in mildly acidic media (pH ~5.4) and in the absence of receptor (and chelators), both sites of hFe_2Tf can fully release bound metal ions only in the presence of ~0.8 M NaCl or ~0.1 M Na_2SO_4 (Figure 1). It is notable that the rate of iron loss from each site of the hFe_2Tf–receptor complex (hFe_2Tf–TR) in mildly acidic medium is controlled by a protonation step and is accompanied by very fast uptake of two protons (Scheme 3).[10] However, in the absence of receptor and in the presence of anions at mildly

dx.doi.org/10.1021/jp205879h | J. Phys. Chem. B 2012, 116, 3795–3807

acidic pH, each site of hFe_2Tf gains one proton in a manner that is kinetically controlled by the interaction with one anion (Scheme 1). The intermediate product resulting from anion binding releases the iron, undergoes two rate-limiting proton transfers, and ultimately releases an anion (Scheme 1).

The proposal of anion binding during iron release is supported by previous reports concerning this family of proteins.[14−19] Wishnia et al. reported electrophoretic and isoionic pH studies consistent with binding of ∼17 chloride ions during iron release from oTf.[17] Folajtar and Chasteen reported that two chloride ions bind to each domain of sTf with strong cooperativity during iron release.[18] These authors found that anions alter the EPR spectrum of the hFe_2Tf complex and suggested that these spectroscopic changes might result from conformational changes induced by anion binding. Notably, recent spectroscopic results provide direct evidence that anion binding to the protein promotes a structural or conformational change around one or more Trp residues near the iron binding sites insofar as anion binding induces a significant blue shift in the fluorescence emission maximum for hFe_2Tf at pH ∼4.2.[85]

Foley and Bates reported that anions promote iron release from hFe_2Tf with an order of effectiveness of $SO_4^{2-} > NO_3^- > Cl^- > ClO_4^-$,[86] an order different from that of the lyotropic series (i.e., an empirical ranking of the relative effectiveness of salt for denaturing or altering the activity of a protein[87,88]). Some other reports also showed that anion effects on iron release do not follow the lyotropic series.[58,89−91] More recently, He et al. reported that at mildly acidic pH, iron release form the isolated N-lobe of sTf is closely related to the anion-binding ability of the protein.[61] At pH ∼4.55, sulfate has a greater effect than chloride or nitrate on iron release from the N- and C-lobes of hFe_2Tf (Figure 3). Because sulfate binds to the protein more strongly than chloride,[16,61] it is possible that in mildly acidic media, iron release from the N- and C-lobes of hFe_2Tf is closely related to the anion binding ability of the protein. Indeed, the affinities of the N- and C-lobes for SO_4^{2-} are about 12.7- and 2.3-fold greater, respectively, than their affinities for Cl^- (Tables 2 and 3).

Table 3. Second Order Rate Constants k_{2C} and Equilibrium Constant K_{2S} at 25.0 (5) °C[a]

anion	k_{2C} (M^{-2} s^{-1})	K_{2S} (M)	K_a (M^{-1})
Cl^-	$8.4(2) \times 10^4$	$1.8(4) \times 10^{-2}$	55.6
SO_4^{2-}	$8.1(1) \times 10^5$	$7.9(2) \times 10^{-3}$	126.6
NO_3^-	$4.4(6) \times 10^5$	$4.6(4) \times 10^{-2}$	22

[a]The uncertainty (standard error) of the least significant figure is indicated in parentheses.

Although the amino acid sequences of the N- and C-lobes of sTf are ∼40% identical, the domains differ in their affinity for iron[37,38] and in their iron binding and release properties.[42−46] The affinity of the C-lobe for iron is well-known to be greater than that of the N-lobe.[25,48] This situation is reflected in the slow rate at which iron is released from the C-lobe as compared to the N-lobe (Figure 2 and Figure 3). In neutral media, "nonchelating" anions such as chloride enhance iron release from the C-lobe while inhibiting iron release from the N-lobe.[51] We did not observe this inhibitory effect of anions on release of iron from the N-lobe at mildly acidic pH because under such conditions the dilysine pair (Lys^{206}-Lys^{296}) and other critical residues would be protonated,[35,61,62,82,92−94] causing two subdomains (NI and NII) to repel each other and induce a "loose" conformation for the N-lobe.[62] This situation enables chloride to enter the iron-binding cleft and to bind to exposed side chains, thereby promoting cleft opening and allowing iron release.

In the absence of an iron chelator, the N-lobe begins to release iron at pH ∼5.7, whereas the C-lobe retains iron to pH ∼4.8.[79,80] This difference may be the consequence of the two structural distinctions between the two lobes of sTf. The first difference involves a pH-sensitive dilysine (Lys^{206}-Lys^{296}) trigger present in the N-lobe that is not present in the C-lobe.[35,59] The second difference concerns the interdomain hydrogen-bonding network in metal-loaded N- and C-lobes of sTf.[32−35] The current results demonstrate that the presence of anions in solution could help to overcome these differences and may allow both sites to release iron at higher pH than they would otherwise. Notably, in the presence of ∼0.1 M sulfate at pH ∼5.4, iron is completely released from both sites (Figure 1).

■ ASSOCIATED CONTENT

Supporting Information

Derivations of the rate expressions for the reciprocal relaxation times used for analysis of the kinetics data reported here. This material is available free of charge via the Internet at http://pubs.acs.org.

■ AUTHOR INFORMATION

Corresponding Author

*Phone: 604-822-3719. Fax: 604-822-6860. E-mail: mauk@interchange.ubc.ca.

Notes

The authors declare no competing financial interest.

■ ACKNOWLEDGMENTS

This work was supported by a Canadian Blood Services-Canadian Institutes of Health Research operating grant (to A.G.M.), a DST SERC grant (to R.K.), a CBS-CIHR Postdoctoral Fellowship (to R.K.), and a Canada Research Chair (A.G.M.). The spectropolarimeter and spectrophotometer were obtained with funds provided by the Canadian Foundation for Innovation to the UBC Laboratory of Molecular Biophysics.

■ REFERENCES

(1) Baker, E. N.; Baker, H. M.; Kidd, R. D. *Biochem. Cell Biol.* **2002**, *80*, 27−84.
(2) Åasa, R.; Malmström, B. G.; Saltman, P. *Biochim. Biophys. Acta* **1963**, *75*, 203−222.
(3) Sun, H.; Li, H.; Sadler, P. J. *Chem. Rev.* **1999**, *99*, 2817−2842.
(4) Tinoco, A. D.; Valentine, A. M. *J. Am. Chem. Soc.* **2001**, *127*, 11218−11219.
(5) Guo, M.; Sun, H.; McArdle, H. J.; Gambling, L.; Sadler, P. J. *Biochemistry* **2000**, *39*, 10023−10033.
(6) Tinoco, A. D.; Incarvito, C. D.; Valentine, A. M. *J. Am. Chem. Soc.* **2003**, *129*, 3444−3454.
(7) Thorstensen, K.; Romslo, I. *Biochem. J.* **1990**, *271*, 1−9.
(8) MacGillivray, R. T. A.; Mason, A. B. Transferrin. In *Molecular and Cellular Iron Transport*; Templeton, D. M., Ed.; Marcel Dekker, Inc.: New York, 2002; pp 41−69.
(9) Dautry-Varsat, A.; Cienchanover, A.; Lodish, H. F. *Proc. Natl. Acad. Sci. U.S.A.* **1982**, *80*, 2258−2262.
(10) Hémadi, M.; Ha-Duong, N. T.; El Hage Chahine, J. M. *J. Mol. Biol.* **2006**, *358*, 1125−1136.
(11) Aisen, P.; Brown, E. B. *Prog. Hematol.* **1975**, *9*, 25−26.

(12) Ling, G. N. *The Aqueous Cytoplasm*; Marcel Dekker: New York, 1979; Vol. *1*, pp 1−230.
(13) Chasteen, N. D. *Iron Binding Proteins Without Cofactors or Sulfur Clusters*; Elsevier: New York, 1983; Vol. *5*; pp 201−233.
(14) Grady, J. K.; Mason, A. B.; Woodworth, R. C.; Chasteen, N. D. *Biochem. J.* **1995**, *309*, 403−410.
(15) Bell, J. D.; Brown, J. C.; Kubal, G.; Sadler, P. J. *Biochem. Soc. Trans.* **1988**, *16*, 714−715.
(16) Harris, W. R.; M., C. A.; Abdollahi, S.; Trankler, K. *Biochim. Biophys. Acta* **1998**, *1383*, 197−210.
(17) Wishnia, A.; Weber, L.; Warner, R. C. *J. Am. Chem. Soc.* **1961**, *83*, 2071−2080.
(18) Folajtar, D. A.; Chasteen, N. D. *J. Am. Chem. Soc.* **1982**, *104*, 5775−5780.
(19) Thompson, C. P.; McCarty, B. M.; Chasteen, N. D. *Biochim. Biophys. Acta* **1986**, *870*, 530−537.
(20) Baker, E. N.; Lindley, P. F. *J. Inorg. Biochem.* **1992**, *47*, 147−160.
(21) Haridas, M.; Anderson, B. F.; Baker, E. N. *Acta Crystallogr.* **1995**, *D51*, 629−646.
(22) Aisen, P.; Listowsky, I. *Annu. Rev. Biochem.* **1980**, *49*, 357−393.
(23) Baker, E. N. *Adv. Inorg. Chem.* **1994**, *41*, 389−463.
(24) Anderson, B. F.; Baker, H. M.; Norris, G. E.; Rice, D. W.; Baker, E. N. *J. Mol. Biol.* **1989**, *209*, 711−734.
(25) Bou-Abdallah, F.; El Hage Chahine, J. M. *Eur. J. Biochem.* **1998**, *258*, 1022−1031.
(26) Bou-Abdallah, F.; El Hage Chahine, J. M. *Eur. J. Biochem.* **1999**, *263*, 912−920.
(27) Anderson, B. F.; Baker, H. M.; Norris, G. E.; Rumball, S. V.; Baker, E. N. *Nature* **1990**, *344*, 784−787.
(28) Kurokawa, H.; Mikami, B.; Hirose, M. *J. Mol. Biol.* **1995**, *254*, 196−207.
(29) Kurokawa, H.; Dewan, J. C.; Mikami, B.; Sacchettini, J. C.; Hirose, M. *J. Biol. Chem.* **1999**, *274*, 28445−28455.
(30) Sharma, A. K.; Rajashankar, K. R.; Yadav, M. P.; Singh, T. P. *Acta Crystallogr. D Biol. Crystallogr.* **1999**, *55*, 1152−1157.
(31) Jeffrey, P. D.; Bewley, M. C.; MacGillivray, R. T. A.; Mason, 5528 A. B.; Woodworth, R. C.; Baker, E. N. *Biochemistry* **1998**, *37*, 13978−13986.
(32) Moore, A. S.; Anderson, B. F.; Groom, C. R.; Haridas, M.; Baker, E. N. *J. Mol. Biol.* **1997**, *274*, 222−236.
(33) Adams, T. E.; Mason, A. B.; He, Q.-Y.; Halbrooks, P. J.; Briggs, S. K.; Smith, V. C.; MacGillivray, R. T. A.; Everse, S. J. *J. Biol. Chem.* **2003**, *278*, 6027−6033.
(34) Baker, H. M.; Anderson, B. F.; Brodie, A. M.; Shongwe, M. S.; Smith, C. A.; Baker, E. N. *Biochemistry* **1996**, *35*, 9007−9013.
(35) Dewan, J. C.; Mikami, B.; Hirose, M.; Sacchettini, J. C. *Biochemistry* **1993**, *32*, 11963−11968.
(36) Pakdaman, R.; Bou-Abdallah, F.; El Hage Chahine, J. M. *J. Mol. Biol.* **1999**, *293*, 1273−1284.
(37) Aisen, P.; Leibman, A.; Zweier, J. *J. Biol. Chem.* **1978**, *253*, 1930−1937.
(38) Lin, L. N.; Mason, A. B.; Woodworth, R. C.; Brandts, J. F. *Biochemistry* **1994**, *33*, 1881−1888.
(39) Shen, Z. M.; Yang, J. T.; Feng, Y. M.; Wu, C. S. *Protein Sci.* **1992**, *1*, 1477−1484.
(40) Lin, L.; Mason, A. B.; Woodworth, R. C.; Brandts, J. F. *Biochem. J.* **1993**, *293*, 517−522.
(41) Oe, H.; Takahashi, N.; Doi, E.; Hirose, M. *J. Biochem.* **1989**, *106*, 858−863.
(42) El Hage Chahine, J. M.; Fain, D. *Eur. J. Biochem.* **1994**, *223*, 581−587.
(43) Marques, H. M.; Walton, T.; Egan, T. J. *J. Inorg. Biochem.* **1995**, *57*, 11−21.
(44) Zak, O.; Aisen, P.; Crawley, J. B.; Joannou, C. L.; Patel, K. J.; Rafiq, M.; Evans, R. W. *Biochemistry* **1995**, *34*, 14428−14434.
(45) Kretchmar, S. A.; Raymond, K. N. *J. Am. Chem. Soc.* **1986**, *108*, 6212−6218.
(46) Zak, O.; Tam, B.; MacGillivray, R. T. A.; Aisen, P. *Biochemistry* **1997**, *36*, 11036−11043.
(47) Bali, P. K.; Harris, W. R. *J. Am. Chem. Soc.* **1989**, *111*, 4457−4461.
(48) MacGillivray, R. T.; Moore, S. A.; Chen, J.; Anderson, B. F.; Baker, H.; Luo, Y.; Bewley, M.; Smith, C. A.; Murphy, M. E.; Wang, Y.; Mason, A. B.; Woodworth, R. C.; Brayer, G. D.; Baker, E. N. *Biochemistry* **1998**, *37*, 7919−7928.
(49) Nurizzo, D.; Baker, H. M.; He, Q. Y.; MacGillivray, R. T.; Mason, A. B.; Woodworth, R. C.; Baker, E. N. *Biochemistry* **2001**, *40*, 1616−1623.
(50) Egan, T. J.; Ross, D. C.; Purves, L. R.; Adams, P. A. *Inorg. Chem.* **1992**, *31*, 1994−1998.
(51) Williams, J.; Chasteen, N. D.; Moreton, K. *Biochem. J.* **1982**, *201*, 527−532.
(52) Baldwin, D. A.; DeSousa, D. M. R. *Biochem. Biophys. Res. Commun.* **1981**, *99*, 1101−1107.
(53) Egyed, A. *Biochim. Biophys. Acta* **1975**, *411*, 349−356.
(54) Pollack, S.; Vanderhoff, G.; Lasky, F. *Biochim. Biophys. Acta* **1977**, *497*, 481−487.
(55) Morgan, E. H. *Biochim. Biophys. Acta* **1979**, *580*, 312−326.
(56) Chasteen, N. D.; Williams, J. *Biochem. J.* **1981**, *193*, 717−727.
(57) Hamilton, D. H.; Turcot, I.; Stintzi, A.; Raymond, K. N. *J. Biol. Inorg. Chem.* **2004**, *9*, 936−944.
(58) Harris, W. R.; Bali, P. K. *Inorg. Chem.* **1988**, *27*, 2687−2691.
(59) Anderson, B. F.; Baker, H. M.; Dodson, E. J.; Norris, G. E.; Rumball, S. V.; Waters, J. M.; Baker, E. N. *Proc. Natl. Acad. Sci. U.S.A.* **1987**, *84*, 1769−1775.
(60) Baker, E. N.; Rumball, S. V.; Anderson, B. F. *Trends Biochem. Sci.* **1987**, *12*, 350−353.
(61) He, Q.-Y.; Mason, A. B.; MacGillivray, R. T. A.; Woodworth, R. C. *Biochemistry* **1999**, *38*, 9704−9711.
(62) He, Q.-Y.; Mason, A. B.; Nguyen, V.; MacGillivray, R. T. A.; Woodworth, R. C. *Biochem. J.* **2000**, *350*, 909−915.
(63) Mizutani, K.; Muralidhara, B. K.; Yamashita, H.; Tabata, S.; Mikami, B.; Hirose, M. *J. Biol. Chem.* **2001**, *276*, 35940−35946.
(64) Muralidhara, B. K.; Hirose, M. *J. Biol. Chem.* **2000**, *275*, 12463−12469.
(65) Chikh, Z.; Hemadi, M.; Miquel, G.; Ha-Duong, N. T.; El Hage Chahine, J. M. *J. Mol. Biol.* **2008**, *380*, 900−916.
(66) Bou-Abdallah, F.; El Hage Chahine, J. M. *J. Mol. Biol.* **2000**, *303*, 255−266.
(67) El Hage Chahine, J. M.; Pakdaman, R. *Eur. J. Biochem.* **1995**, *230*, 1102−1110.
(68) Egan, T. J.; Zak, O.; Aisen, P. *Biochemistry* **1993**, *32*, 8162−8167.
(69) He, Q. Y.; Mason, A. B.; Woodworth, R. C.; Tam, B. M.; Wadsworth, T.; MacGillivray, R. T. *Biochemistry* **1997**, *36*, 5522−5528.
(70) Mason, A.; He, Q. Y.; Tam, B.; MacGillivray, R. A.; Woodworth, R. *Biochem. J.* **1998**, *330* (Pt1), 35−40.
(71) Bates, G. W.; Schlabach, M. R. *J. Biol. Chem.* **1973**, *248*, 3228−3232.
(72) van Renswoude, J.; Bridges, K. R.; Harford, J. B.; Klausner, R. D. *Proc. Natl. Acad. Sci. U.S.A.* **1982**, *79*, 6186−6190.
(73) He, Q. Y.; Mason, A. B.; Pakdaman, R.; Chasteen, N. D.; Dixon, B. K.; Tam, B. M.; Nguyen, V.; MacGillivray, R. T.; Woodworth, R. C. *Biochemistry* **2000**, *39*, 1205−1210.
(74) Mason, A. B.; Halbrooks, P. J.; Larouche, J. R.; Briggs, S. K.; Moffett, M. L.; Ramsey, J. E.; Connolly, S. A.; Smith, V. C.; MacGillivray, R. T. *Protein Expr. Purif.* **2004**, *36*, 318−326.
(75) Eigen, M.; deMaeyer, L. Relaxation Methods. In *Techniques of Organic Chemistry*; Friess, S. L., Lewis, E. S., Weissberger, A., Eds.; Interscience: New York, 1963; Vol. *8* (pt. 2), pp 895−1029.
(76) Brouillard, R. *J. Chem. Soc., Faraday Trans.* **1980**, *76*, 583−587.
(77) Pitzer, K. S. *J. Phys. Chem. B* **1973**, *77*, 268−277.
(78) Pitzer, K. S. *Acc. Chem. Res.* **1977**, *10*, 371−377.
(79) Princiotto, J. V.; Zapolski, E. J. *Nature* **1975**, *255*, 87−88.
(80) Baldwin, D. A.; De Sousa, D. M.; Von Wandruszka, R. M. *Biochim. Biophys. Acta* **1982**, *719*, 140−146.
(81) Cheng, Y.; Mason, A. B.; Woodworth, R. C. *Biochemistry* **1995**, *34*, 14879−14884.

(82) Beatty, E. J.; Zhong, W.; Kubal, G.; Houldershaw, D.; Goodfellow, J. M.; Sadler, P. J. *J. Inorg. Biochem.* **2002**, *88*, 403−409.
(83) Bernasconi, C. F. *Relaxation Kinetics*; Academic Press: New York, 1976.
(84) Bali, P. K.; Zak, O.; Aisen, P. *Biochemistry* **1991**, *30*, 324−328.
(85) Kumar, R.; Mauk, A. G. *J. Phys. Chem. B* **2009**, *113*, 12400−12409.
(86) Foley, A. A.; Bates, G. W. *Biochim. Biophys. Acta* **1988**, *965*, 154−162.
(87) Record, M. T.; Anderson, C. F.; Lohman, T. M. *Q. Rev. Biophys.* **1978**, *11*, 103−178.
(88) Cacace, M. G.; Landau, E. M.; Ramsden, J. J. *Q. Rev. Biophys.* **1997**, *30*, 241−277.
(89) Baldwin, D. A. *Biochim. Biophys. Acta* **1980**, *623*, 183−198.
(90) Marques, H. M.; Watson, D. L.; Egan, T. J. *Inorg. Chem.* **1991**, *30*, 3758−3762.
(91) Li, Y.; Harris, W. R. *Biochim. Biophys. Acta* **1998**, *1387*, 89−102.
(92) Messori, L.; Poggetto, G. D.; Monnanni, R.; Hirose, J. *Biometals* **1997**, *10*, 303−313.
(93) Lee, D.; Goodfellow, J. *Biophys. J.* **1998**, *74*, 2747−2759.
(94) Rinaldo, D.; Field, M. J. *Biophys. J.* **2003**, *85*, 3485−3501.